Computer-simulation study of melting in dense oxygen layers on graphite

Venkat R. Bhethanabotla* and William A. Steele
Department of Chemistry, The Pennsylvania State University, University Park, Pennsylvania 16802
(Received 5 July 1989)

The thermodynamic, structural, and dynamical properties of oxygen adsorbed on graphite have been simulated using a molecular-dynamics algorithm. The simulations were run at temperatures ranging from 30 to 70 K and at nominal coverages of one (dense) layer, ~1.7 layers, two layers, and three layers. Melting behavior was characterized in all cases. Enthalpies, layer densities (solid and liquid), and temperatures of melting were obtained. The temperature for first-layer melting was found at 55–60 K and was not very dependent upon total coverage. This melting appeared to be sharp for most cases studied. Second-layer melting behavior depended very strongly on the layer density, and compound liquid-solid layers were observed. The simulation results are found to be in good agreement with experiment. The importance of orientational changes in determining the properties of these systems is demonstrated and discussed.

I. INTRODUCTION

The structural and thermodynamic properties of O_2 physisorbed on the graphite basal plane have been extensively studied.[1–29] This is partly due to the fact that, in spite of the similarities in size, shape, and interaction energy between O_2 and N_2, the phase diagrams for these molecules adsorbed on graphite show pronounced differences.[8,21] At temperatures below ~20 K, the magnetic interactions in O_2 give rise to an ordered phase which is, of course, absent in N_2. Above this temperature, the quadrupolar interactions in N_2 are an important source for the differences with O_2, which has a relatively small quadrupole moment. If one neglects magnetic interaction terms, it is straightforward to produce realistic models for the interaction potentials in the O_2/graphite system[27,28] which can then be used in a variety of calculations, including computer simulation studies at $T > 20$ K. In this paper such simulations are reported for four coverages ranging from monolayer to trilayer at temperatures ranging from below the melting points to considerably above. We find considerable changes in the layer properties as the temperature changes, including alterations in the monolayer density which produce significantly different coverages (measured in layers) as the temperature increases.

One of the striking differences between O_2 and N_2 monolayers on graphite at low temperatures is the larger compressibility of the two dimensional (2D) O_2 solid. The lowest-density solid observed has a centered-rectangular lattice with a density of ~0.073 $Å^{-2}$ and a melting point of ~26 K (δ phase). As more molecules are added to the system, the solid changes symmetry and density to one of several ζ phases which differ primarily in their orientation relative to the underlying graphite lattice. They are characterized by a density of ~0.08 $Å^{-2}$ (at its lowest limit—some compression is possible). As density increases even more, a lattice forms in which molecular orientation relative to the surface has shifted from almost surface-parallel (observed in the low-density phase) to angles approaching those for surface-perpendicular orientation. The melting point of this phase depends upon its density but is definitely higher than that for the δ phase. Among the questions investigated in the present study are what is the melting point of this monolayer, and what happens when a second and/or third layer of O_2 is added to this system? We will show that the results of the simulations presented here are in good agreement with recent experimental work in this region of the phase diagram.

II. SIMULATION

The details of the potential energies for O_2-O_2 and O_2-graphite interactions have been given elsewhere[27,28,30] and will not be repeated here. The models are based on site-site representations of both O_2 and graphite. Well-depth and size parameters for the 12-6 potential functions used are shown in Table I. The resulting energies include reasonably realistic representations of the shape of an oxygen molecule as well as the periodicity of the gas-solid potential. Classical molecular dynamics simulations were carried out using a fourth-order predictor-corrector algorithm based on the quaternion representation of molecular orientation,[31] and a time step of 4.9×10^{-3} psec. Constant-temperature dynamics were found to be essential to avoid the large jumps in temperature that would otherwise occur whenever a molecule switched adsorbed layers—this happens regularly in the high-temperature runs of these calculations (i.e., 60 K and above). The Evans-Hoover isokinetic algorithm[32] was used to avoid such jumps. (Although this choice rather than the Nosé or Andersen algorithms is arguable, it does have the advantage of precisely eliminating all fluctuations in the temperature no matter how short the time interval.)

Simulations were carried out at various temperatures for four different O_2 coverages. Run 1 is made up of data taken at nine temperatures ranging from 35 to 85 K at a coverage of roughly 1.7 layers (see below). The number of temperatures for runs 2 and 3 are more limited, in part because the interesting range had been determined in run 1. Thus, five temperatures ranging from 35 to 65 K and

TABLE I. Parameters of the site-site potentials.

Sites	ε/k (K)	σ (Å)
O-O	52.1	2.99
O-C	38.2	3.195
	$u_{ss}=4\varepsilon[(\sigma/r)^{12}-(\sigma/r)^{6}]$	

an approximate coverage of one layer were taken in run 2, and six temperatures over the range 45 to 65 K at a coverage of two layers were taken in 3. Run 4 consisted in simulations at six temperatures for a nominal trilayer coverage. Some difficulties were encountered in achieving complete equilibrium at the lowest temperatures. In particular, at $T<45$ K, the first-layer center-of-mass packing can remain at a metastable value because of the slow rate of molecular exchange in and out of these 2D solid layers.

Figure 1 summarizes the "equilibrium" densities observed for three runs. At temperatures less than 60 K, the first-layer densities for these runs are only approximately equal, ranging from 0.107 to 0.112 Å^{-2}. We believe that these small differences are more a reflection of lack of equilibrium than of any real effect. Also, runs 1 and 3 give essentially complete first and second layers for $T>60$ K with nearly equal but temperature-dependent densities. The value at 65 K is 0.076 Å^{-2} (± 0.002). The sharp expansion of the first layer observed at 60 K occurs by promotion of molecules to the third layer for runs 1 and 3 and to the second layer for run 2. We will show that the transition at 60 K is due to first-layer melting accompanied by a significant change in orientational order.

The numbers of molecules and the simulation box size varied from run to run. In run 1, the initial configuration was taken to be 120 O_2 molecules in the first layer in a box of dimensions $16\times 6\sqrt{3}$ (reduced units for length are obtained by dividing length in Å by 2.46 Å) and 72 molecules in the second. The first layer was initially chosen to be triangular with all molecules perpendicular to the surface; the second was set in a configuration which is centered rectangularly with all molecules parallel to the surface. After equilibration at the lowest temperature, the system stabilized with 112 molecules in layer 1 and 80 in layer 2.

In runs 2–4, 72 molecules were placed in the first layer in the same structure as for run 1 but in a box of dimensions $8\times 8\sqrt{3}$. Run 2 was initially a single monolayer. Run 3 was initially taken to be two layers thick with the outer identical to the first, and run 4 was initially set at three identical layers.

Each run consisted of a series of simulations performed at successively higher temperatures. In this way, one could take the final configuration from the previous simulation to be the initial configuration for the simulation at the next higher temperature. (Obviously, the initial configurations described above refer only to the simulation at the lowest temperature for a given run.) At $T\geq 45$ K, we judged that sufficient time steps had been taken to achieve equilibration, with the possible exception of deviations from the equilibrium value of the first-layer density at $T<60$ K. Subsequent to the equilibration period, molecular configurations and thermodynamic data were recorded.

The calculations include average potential energies per molecule in a given layer but these energies were further subdivided into $\langle u_{gs}(n)\rangle$ the average molecule-solid energy for a molecule in layer n, $\langle u_{mm}(i)\rangle$ the average energy of an O_2 molecule in layer i interacting with molecules in the same layer, and $\langle U_{mm}(ij)\rangle$ the total energy of interaction between layers i and j. In addition, orientational distributions were simulated for the molecules in each of the layers. A number of orientational time-correlation functions were evaluated that were useful in characterizing orientational ordering. It was found to be helpful to make computer-generated plots of the time-dependent trajectories of the molecular centers-of-mass in the plane of the layer, since one can use them to obtain a reasonably good feel for the presence of solid (oscillations about lattice points) or a fluid (diffusive displacements) as temperature varies.

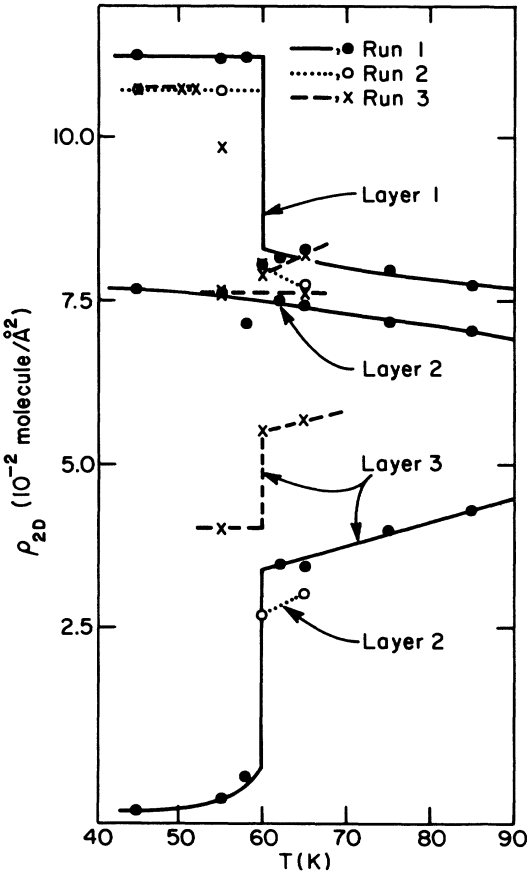

FIG. 1. Layer densities are shown as a function of temperature for runs 1, 2, and 3. The low-temperature densities for layer 1 are roughly 0.106 molecule/Å^2 and hardly vary with total coverage, for the values used here. The sharp drop at ~ 60 K is associated with melting to a liquid layer of density ~ 0.080 molecule/Å^2. Observed second-layer densities vary smoothly with temperature and appear to be those for a 2D liquid (except for run 2, where the layer is incomplete). The third layers are all partially filled, with densities that reflect this fact.

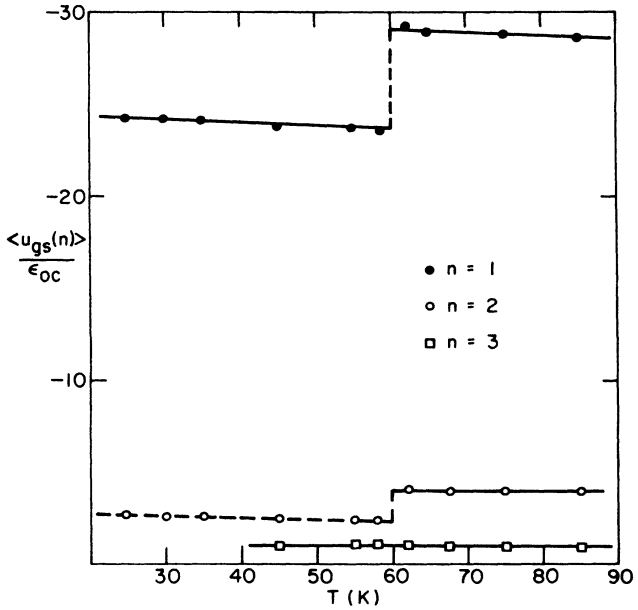

FIG. 2. The average gas-solid potential energy per O_2 for the molecules in the separate layers (denoted by n) in run 1.

III. RESULTS

We begin with the plots of average gas-solid potential energy per particle shown in Fig. 2. For run 1, it is clear that the gradual change of this energy with temperature is abruptly altered in the region between 58 and 62 K. For first-layer molecules, the most obvious possibility for this break is that molecular orientation relative to the surface is altered and this idea is confirmed by plots shown in Fig. 3 for the distribution of $\cos\beta$ at temperatures above and below the transition region. In addition, the surface-averaged center-of-mass density $f(z^*)$ is shown for two temperatures in Fig. 4. The sharp peak in $P(\cos\beta)$ at 55 K which corresponds to a predominance of molecules oriented perpendicular to the surface is replaced by a rather broad function at 65 K that shows a large fraction of molecules nearly parallel to the surface. When plotted as a function of center-of-mass distance, the model gas-solid potential for a dumbbell-shaped molecule such as O_2 has minima whose values and positions change significantly with orientation. The shift in the position of the maximum density for layer 1 (shown in Fig. 4) in going from 55 to 65 K and the appearance of a shoulder in the peak are quite consistent with an orientational change from nearly all perpendicular at 55 K, with a minimum in energy and maximum in $f(z^*)$ occurring at $z^*=1.5$ ($z=3.7$ Å), to a layer with both surface-parallel having center-of-mass position at $z^*=1.3$ ($z=3.2$ Å) and perpendicular molecules. Furthermore, one imagines that the projected area of a freely rotating surface-parallel molecule will be noticeably larger than that for a perpendicular molecule. Consequently, the monolayer, which is nearly close-packed above and below the transition, must undergo a significant density change when the orientation changes as indicated. Such a density change is shown quite clearly in Fig. 1. It is interesting to note that the second-layer density does not shift much across this temperature interval so that one must conclude the molecules lost to the first layer must go into layer three. Figure 4 confirms this while also showing that the position of layer three relative to the surface is rather smeared out. This is easy to understand, since the holding potential for these molecules is a combination of a small and slowly varying gas-solid energy at these distances plus the interaction of third-layer molecules with the underlying first- and second-layer molecules. Of course the O_2-O_2 energy has significant fluctuations due to orientional and positional motion in the underlayers, which in turn produces a distribution of the third-layer properties including distance from the surface.

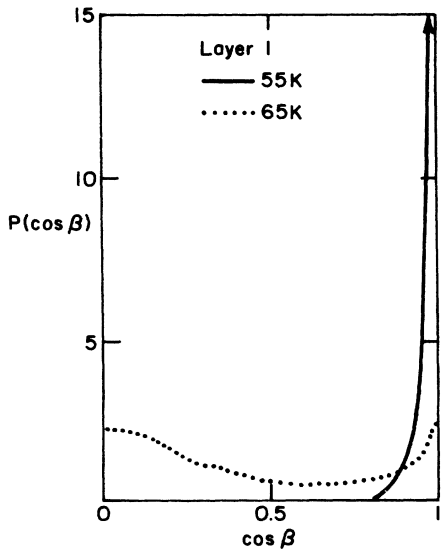

FIG. 3. Distributions for the cosine of the molecular axis orientation β relative to the normal to the surface are shown for O_2 in the first layer of run 1 at 55 and at 65 K.

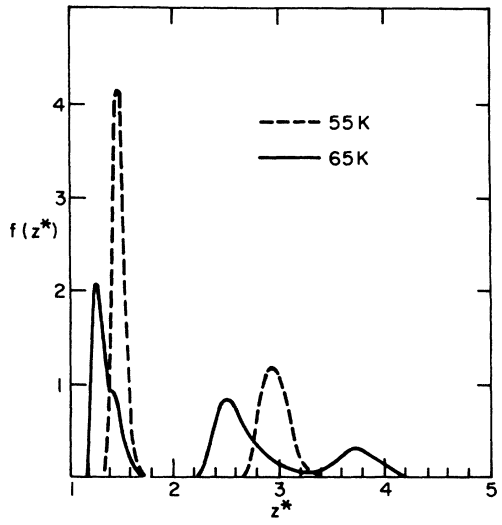

FIG. 4. Distributions of the center-of-mass distance z^* from the surface are given here for run 1 at two temperatures. Reduced units for z are defined as $z^*=z/2.46$ Å.

Although some change in the molecular orientational distributions occurs in the second layer in going from 55 to 65 K, as shown in Fig. 5, it is clear that the primary reason for the change in average gas-solid energy shown in Fig. 2 for a molecule in this layer is actually due to the shift in average molecule-solid separation distance rather than a change in molecular orientation. This unexpected result has interesting implications for theories which commonly assume fixed distances and gas-solid energies for the molecules in a given layer of a multilayer film.

Figure 6 gives the average gas-solid energies for first-layer molecules at the coverages of runs 2 and 3. (The data from run 1 are shown by dashed lines for comparison purposes.) Although these results are not as detailed as those for run 1, they do show a jump in the 55–60 K region for layer 1. In the case of run 2, a jump from essentially no second-layer molecules to a roughly 0.3 coverage at $T \cong 55$ K was found—consequently, no second layer data exists at $T < 55$ K. The curves of density versus distance from the surface that are shown in Fig. 7 confirm the fact that these systems are quite similar to run 1 in that a first-layer melting accompanied by orientational change from perpendicular to a mix of orientations occurs at temperatures around 55–60 K.

We now consider the simulated values of the average O_2-O_2 energies per molecule. The data for intralayer energies are shown in Fig. 8 for all three runs. Significant jumps are observed in the 55–60 temperature interval, with the first layer becoming less stable in all cases. It is not surprising to find a loss of O_2-O_2 stabilization energy in layer 1, since the orientational change in this temperature range clearly produces an over-compressed layer which relieves part of the compression by expelling molecules, as seen by the sharp decrease in density in Fig. 1.

There appears to be no simple explanation for the jump in second-layer O_2-O_2 energy. The results shown in Fig. 1 indicate that density of this layer varies smoothly with temperature. Furthermore, the curves of Fig. 5 show only a small change in out-of-plane orientational distribution. So far as the average O_2-O_2 interaction goes, the most significant change in second-layer properties between 55 and 60 K is the broadening of distribution of

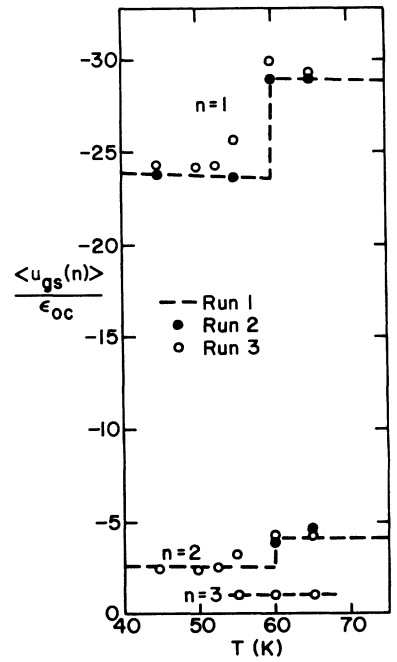

FIG. 6. Same as Fig. 2, but the points show results for runs 2 and 3.

the molecule-surface distances shown in Figs. 4 and 7. Whether it is this alteration that is responsible for the net increase in attractive energy within this layer is not known.

Additional support for first-layer melting near 60 K is obtained from the computed time-dependent center-of-mass trajectories for the sample of molecules. Figure 9 shows a top view of the trajectories followed by the first-layer molecules over a 50 psec time interval in run 1. It is clear that this layer is solid at 58 K and fluid at 62 K. Figure 10 shows the same trajectories for molecules in the second layer of run 1 at several temperatures. These plots lead to the conclusion that for this layer density, layer 2 melts at a low temperature of approximately 30–40 K. Note that the low-density δ monolayer solid is known to melt at 28 K. Since the density of the layer of

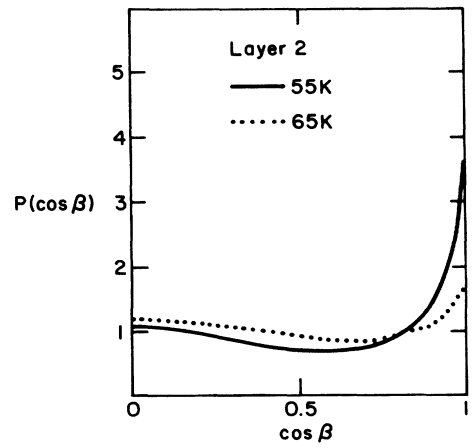

FIG. 5. Same as Fig. 3, but for the second-layer molecules.

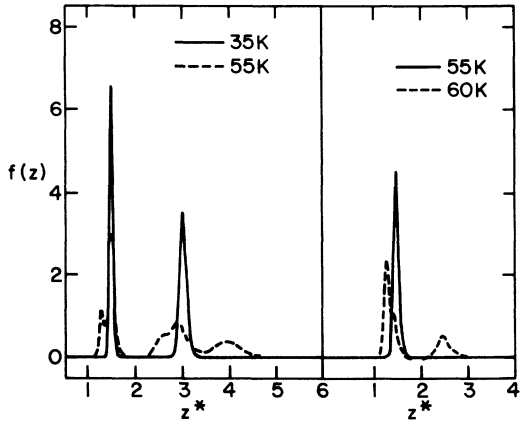

FIG. 7. Same as Fig. 4, but results for run 3 are shown in the left-hand panel while those for run 2 are shown on the right.

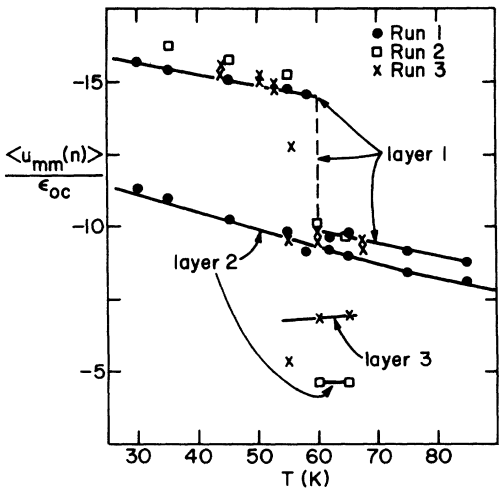

FIG. 8. Intralayer energies are shown here as a function of temperature. The quantity $u_{mm}(n)$ in the average O_2-O_2 potential energy for a molecule in layer n interacting with the other molecules in the same layer. The pairs of crosses are for the first and the second layers.

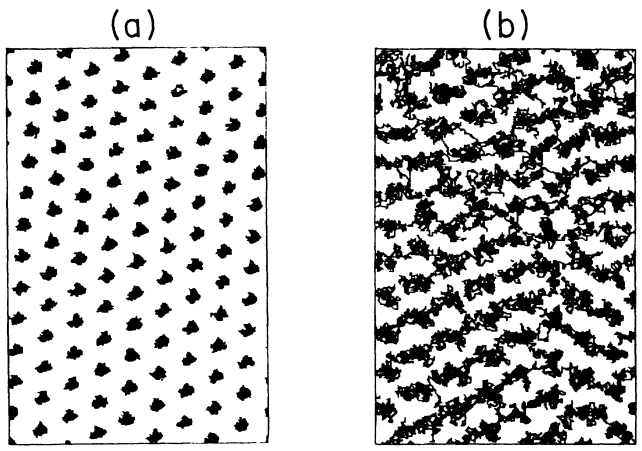

FIG. 9. Computer-generated trajectories for the center-of-mass motion parallel to the plane of the surface. These are shown for a time interval of ~50 psec for all the molecules in the first layer of run 1. Plots are for 58 K (a) and 62 K (b)—just below and just above the melting point.

Fig. 9 (0.075 $Å^{-2}$) is comparable to the δ solid (0.073 $Å^{-2}$), similar behavior of the two layers is not surprising.

Figure 11 shows time-correlation functions for the first layer of run 2 at two temperatures near the transition. Two types of function are shown: one that measures that change in the angle β between the molecular axis and the normal to the surface by evaluating

$$C_1^{(\text{out})}(t)=\langle \cos\delta\beta \rangle \ , \tag{1}$$

where $\delta\beta$ is the change in β in time interval t and the brackets denote an average over molecules and over starting times in the computer simulation. The uppermost curve shows that $\delta\beta$ remains small at 55 K and $C_l^{(\text{out})}(t)$ corresponds to an ensemble of librators, as one might expect for a layer in which all molecules are nearly perpendicular to the surface. The slow decay seen in $C_1^{\text{out}}(t)$ at 60 K, indicates that some reorientation is possible, again in agreement with a picture in which melting is accompanied by a change in the out-of-plane orientational order.

The dashed curves in Fig. 11 give time-correlation functions for the in-plane angle α. Specifically,

$$C_1^{(\text{in})}(t)=\langle \cos\alpha \rangle \ , \tag{2}$$

where α is the angle between the in-plane projections of the molecular axis at time zero and at time t. The oscillatory behavior at 55 K is characteristic of in-plane libration whereas the roughly exponential curve for 60 K is characteristic of the rotational diffusion expected in a liquid layer.

The trajectories and time-correlation-functions in Figs. 12 and 13 respectively show a more complex situation for the first layer of the two-layer system of run 3 than for run 2. The trajectories for the first layer at 55 K may be interpreted as those for a partially liquefied solid layer. The corresponding results at 65 K are somewhat ambiguous but appear to indicate complete liquefaction. The out-of-plane time-correlation-functions in Fig. 13 are decaying slowly for all temperatures. The in-plane functions are more interesting, since they indicate rotational

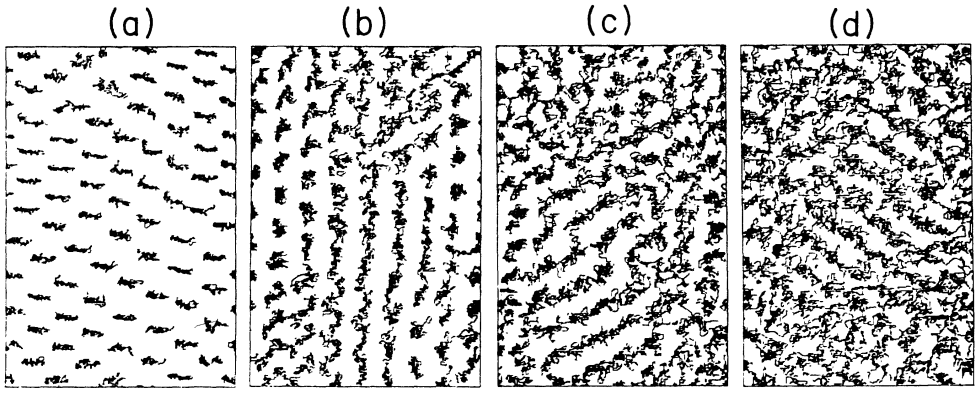

FIG. 10. Same as Fig. 9, but for the molecules in layer 2 at 25 K (a), 35 K (b), 45 K (c), and 55 K (d).

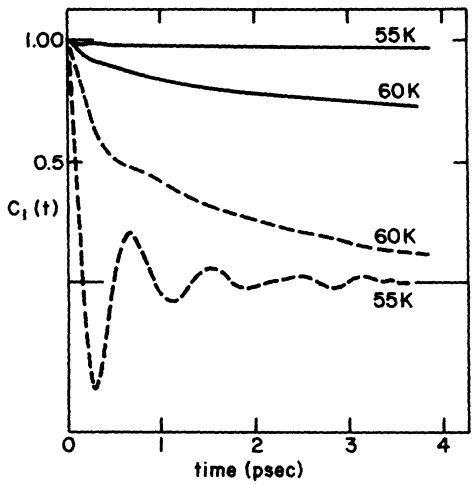

FIG. 11. Time-correlation-functions for the out-of-plane (solid curves) and in-plane (dash curves) reorientational motions for the first-layer molecules of (the monolayer) run 2. These functions are defined by Eqs. (1) and (2) in the text.

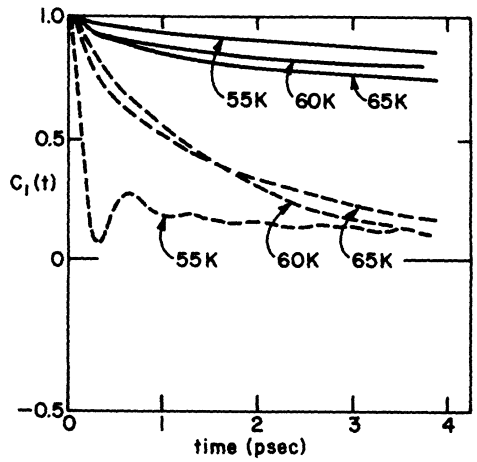

FIG. 13. Same as Fig. 11, but for molecules in the first layer of run 3.

diffusion at 60 and 65 K, but some distinctly different motion at 55 K. The initial oscillations in the 55 K curve are expected for oscillatory motion in an ordered phase, but do not approach zero as in Fig. 11. It is plausible to suppose that the layer is a mix of the highly hindered molecules in a solid region and molecules undergoing slow in-plane rotational diffusion (which might account for the slow approach to zero).

Figure 14 shows densities for the trilayer system as a function of distance from the surface. The temperatures of these curves were chosen to be in the melting region. We associate changes in layer density and layer position with melting plus randomization of orientations. For $T=50$, 55, and 65 K, the layer densities in these systems are: 0.107, 0.107, and 0.080 for layer 1; 0.107, 0.076, and

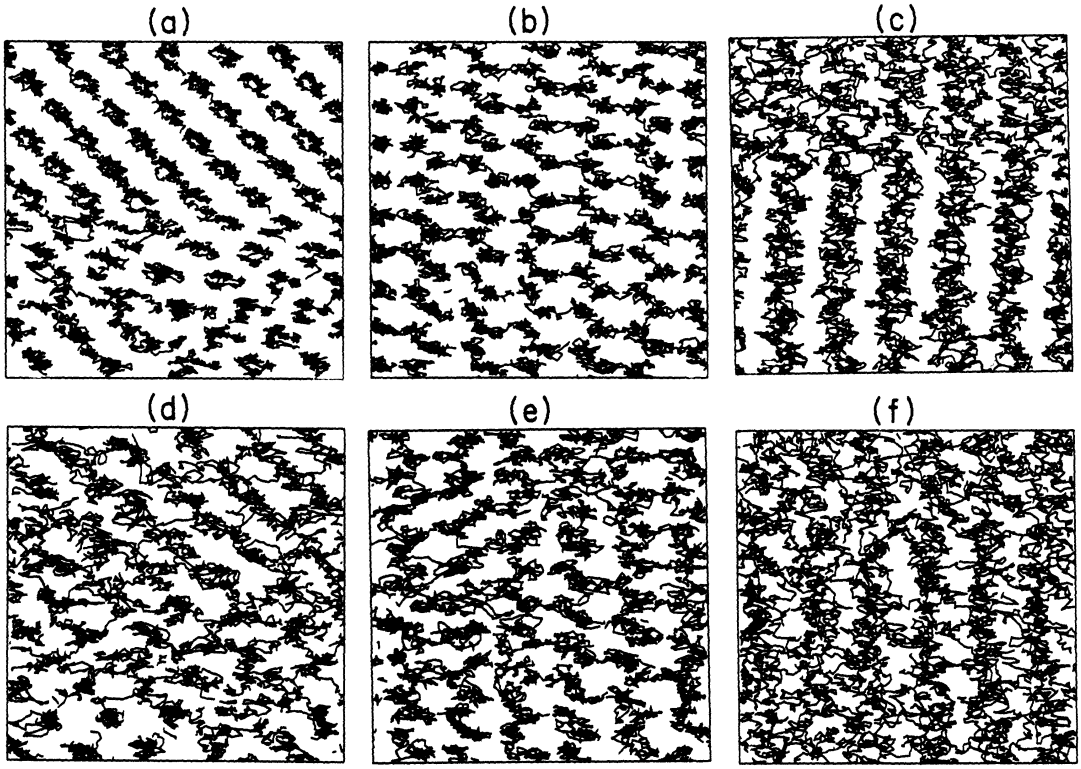

FIG. 12. Center-of-mass trajectories for the molecules in the first two layers of (the bilayer) run 3 are plotted for intervals of ~50 psec at 55 K (a), 60 K (b), and 65 K (c) and at the same temperatures for layer 2 (d)–(f).

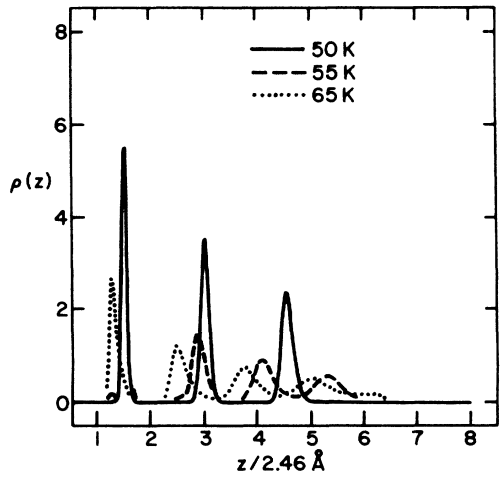

FIG. 14. Center-of-mass densities are shown for the trilayer system (run 4) as a function of molecule-surface separation. The shifts in peak positions and the changes in peak area are associated with layer melting.

0.077 for layer 2; and 0.107, 0.070, and 0.074 for layer 3. These results plus the shifts in peak position shown in Fig. 14 and associated with orientational randomization lead to the conclusion that layers 2 and 3 melt in the range between 50 and 55 K, whereas layer 1 melts somewhere between 55 and 65 K. It is reasonable to suppose that some coupling exists between these close transitions and that the somewhat gradual change in energy shown in Fig. 15 for this temperature region would reflect such coupling.

IV. DISCUSSION

The simulations presented here agree nicely with the current experimental data. For example, compound

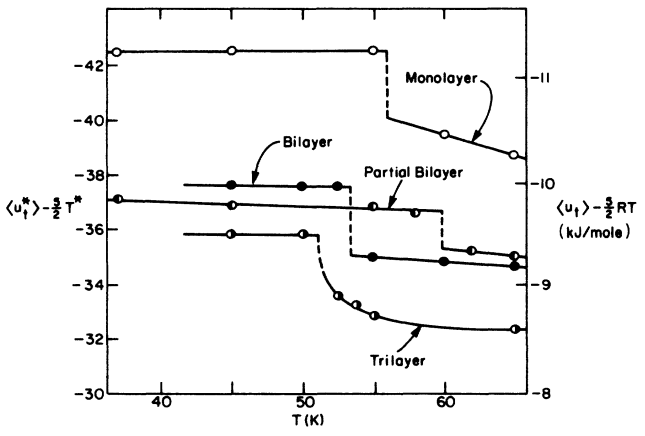

FIG. 15. The average total potential energies of the simulated systems are plotted as a function of temperature. The harmonic vibration-libration thermal energy has been subtracted from the averages in an attempt to accentuate the jumps in energy associated with layer melting. Dashed vertical lines indicate approximately where this melting is believed to occur. For the monolayer and the partial bilayer, first layer-melting is observed; for the bilayer and trilayer cases, it appears that all layers melt at nearly the same temperature.

solid-liquid films have been suggested by several workers and have been proven to exist by neutron scattering experiments[29] which also gave 0.11 molecules/Å^2 for the 2D solid-layer density in bilayer and trilayer films. However, observed melting temperatures tend to be lower than those found in this simulation. For example, the dense monolayer melts at 48±1 K rather than the 55–60 K estimate made here. There are several likely contributing factors to this discrepancy: First, we have not attempted to correct the first-layer O_2-O_2 potential functions for substrate mediated effects,[30] which are known to reduce well depths by 15–20 %. In effect, this means that our transition temperatures are about 15–20 % too high. Second, experimental melting points are quite sensitive to density, as has been shown for N_2 and Kr on graphite for example. This problem is especially significant at the high layer packings. Also, the simulations suffer somewhat from lack of complete translational equilibrium at low temperature. It is quite possible that the solid layers of the simulation are slightly overcompressed which would tend to raise their melting points. The neutron diffraction experiments on bilayer and trilayer films are inconclusive as to the nature of this melting; our results suggest that the first-layer transitions may be distinct. However, this behavior may also be a consequence of the exact coverages chosen. That is, we see that melting in this system is accompanied by layer promotion and significant orientational changes. In this case, the conditions for a first-order thermodynamic transition are not always fulfilled because the chemical potential of the molecules in the outermost liquidlike layer is continuously changing as the transition proceeds. (This would be the case even in a gedanken melting experiment performed at constant temperature.) In principle, the only exception occurs for submonolayer melting of a partly covered surface. Depending upon the particular value of the coverage chosen and upon the magnitude of the melting density change, the actual smearing out of the transition may vary over a considerable range of temperature. In the present case, the layer density change is in excess of 30% (from 0.11 to 0.075 molecules/Å^2) so one might expect to see transitions occurring over a considerable range of temperature even if they were sharp when run under the appropriate conditions. Plots of the temperature dependence of total potential energy of each of the systems simulated are given in Fig. 15. These indicate that the transitions, which now have been shown to be first-layer melting from trajectories and other data, are rather sharp, occurring over a range narrower than 5 K. However, it is interesting to note that the trilayer results indicate smearing of the transition over a 5 K range. (Satisfactory simulations very close to first-order transitions are difficult because of long equilibrium times and large fluctuations.) One can estimate energies of melting from the lengths of the dashed lines in Fig. 15. This is essentially constant and is equal to 0.6 kJ/mole for monolayer and bilayer systems and for the trilayer as well, if one makes a linear extrapolation of the high temperature data. The energy change is about 0.4 kJ/mole for the partial bilayer. Obviously, all values are subject to significant uncertainty, especially if the transitions are

not sharp. The energetics of "layer melting" in these systems is actually very complex, involving changes in O_2-solid energy as well as O_2-O_2 energies of all layers. To take a specific example, the total reduced energy changes between 58 and 62 K for the partially complete bilayer composed of 192 molecules may be broken down as follows: changes in O_2-solid energy due to reorientational and positional shifts: within layer 1, -459; in layer 2, -121; in layer 3, 0; changes in O_2-solid energy due to gain or loss of molecules within a layer: layer 1, $+730$; layer 2, -8; layer 3, -30; changes in O_2-O_2 energy due to reorientational and positional shifts: layer 1, $+408$; layer 2, -7; layer 3, -31; changes in O_2-O_2 energy due to population changes: layer 1, $+449$; layer 2, -31; layer 3, -151; changes in interlayer O_2-O_2 energy: layer 1 with 2, -41; layer 1 with 3, -34 layer 2 with 3, -368. Thus, the change in the total O_2-solid energy is $+271$ (layer 1) -128 (layer 2) -30 (layer 3)$=+113$; the change in the total O_2-O_2 energy is $+857$ (layer 1) -38 (layer 2) -185 (layer 3) -443 (between different layers)$=+191$. Consequently, the net energy change is $+304$ or $15.5.10^{-23}$ kJ. It is obviously impossible to associate this final number with the changes occurring within layer 1 even though the basic cause is melting within that layer. Indeed, a calculation of this layer energy of melting is ambiguous since one does not know whether to calculate on the basis of the total molecules in the film, giving $\Delta U_m = 0.49$ kJ/mol, or the molecules initially in layer 1 (59%), giving $\Delta U_m = 0.83$ kJ/mole. Similar complications arise in all systems studied here.

The primary advantage of the simulations reported here is the detailed information gained concerning the orientational properties of molecules in these films. There is no direct experimental information available bearing on this point, although some of the interpretations of the diffraction data are based on packing concepts that require perpendicular molecules in the densest solid layers.[10,13,29]

ACKNOWLEDGMENTS

V. R. Bhethanabotla thanks Engineering Computing of the University of South Florida for providing him with computational facilities. The work carried out at Penn State was supported by a grant from the Division of Materials Research of the National Science Foundation.

*Present address: Department of Chemical Engineering, University of South Florida, Tampa, FL 33620.

[1]J. Dericbourg, Surf. Sci. **59**, 554 (1976).
[2]J. P. McTague and M. Nielsen, Phys. Rev. Lett. **37**, 596 (1976).
[3]R. D. Etters, R.-P. Pan, and V. Chandrasekharan, Phys. Rev. Lett. **45**, 645 (1980).
[4]M. Nielsen and J. P. McTague, Phys. Rev. B **19**, 3096 (1979).
[5]J. Stoltenberg and O. Vilches, Phys. Rev. B **22**, 2920 (1980).
[6]P. W. Stephens, P. A. Heiney, R. J. Birgeneau, P. M. Horn, J. Stoltenberg, and O. Vilches, Phys. Rev. Lett. **45**, 1959 (1980).
[7]R.-P. Pan, R. D. Etters, K. Kobashi, and V. Chandrasekharan, J. Chem. Phys. **77**, 1035 (1982).
[8]S. C. Fain, Jr., M. F. Toney, and R. D. Diehl, in *Proceedings of the Ninth International Vacuum Congress and Fifth International Conference on Solid Surfaces, Madrid, 1983,* edited by J. L. Segovia (Imprenta Moderna, Madrid, 1983).
[9]M. F. Toney, R. D. Diehl, and S. C. Fain, Jr., Phys. Rev. B **27**, 6413 (1983).
[10]P. A. Heiney, P. W. Stephens, S. G. J. Mochrie, J. Akimitsu, R. J. Birgeneau, and P. M. Horn, Surf. Sci. **125**, 539 (1983).
[11]D. D. Awshalom, G. N. Lewis, and S. Gregory, Phys. Rev. Lett. **51**, 586 (1983).
[12]R. D. Etters and K. Kobashi, J. Chem. Phys. **81**, 6249 (1984).
[13]S. G. J. Mochrie, M. Sutton, J. Akimitsu, R. J. Birgeneau, P. M. Horn, P. Dimon, and D. E. Moncton, Surf. Sci. **138**, 599 (1984).
[14]C. E. Bartosch and S. Gregory, Phys. Rev. Lett. **54**, 2513 (1985).
[15]R. Marx and B. Christoffer, J. Phys. C **18**, 2849 (1985).
[16]Y. P. Joshi and D. J. Tildesley, Surf. Sci. **166**, 169 (1986).
[17]H. You and S. C. Fain, Jr., Phys. Rev. B **33**, 5886 (1986).
[18]M. Drir and G. B. Hess, Phys. Rev. B **33**, 4758 (1986).
[19]S. Tang, S. D. Mahanti, and R. K. Kalia, Phys. Rev. Lett. **56**, 484 (1986).
[20]K. Flurchick and R. D. Etters, J. Chem. Phys. **84**, 4657 (1986).
[21]M. F. Toney and S. C. Fain, Jr., Phys. Rev. B **36**, 1248 (1987).
[22]O. M. B. Duparc and R. D. Etters, J. Chem. Phys. **86**, 1020 (1987).
[23]D. Kirin, B. Kuchta, and R. D. Etters, J. Chem. Phys. **87**, 2332 (1987).
[24]R. Marx and B. Christoffer, Phys. Rev. B **37**, 9518 (1988).
[25]J. Krim, J. P. Coulomb, and J. Bouzidi, Phys. Rev. Lett. **58**, 583 (1987).
[26]K. Morishigi, K. Mimata, and S. Kittaka, Surf. Sci. **192**, 197 (1987).
[27]V. Bhethanabotla and W. A. Steele, Langmuir **3**, 581 (1987).
[28]V. Bhethanabotla and W. A. Steele, Can. J. Chem. **66**, 866 (1988).
[29]R. Chiarello, J. P. Coulomb, J. Krim, and C. L. Wang, Phys. Rev. B **38**, 8867 (1988) (references to previous work are given therein); R. Chiarello and J. Krim, Langmuir **5**, 587 (1989).
[30]M. J. Bojan and W. A. Steele, Langmuir **3**, 116 (1987).
[31]M. P. Allen and D. J. Tildesley, *Computer Simulation of Liquids* (Clarendon, Oxford, 1987).
[32]D. J. Evans and G. P. Morriss, Comput. Phys. Rep. **1**, 297 (1984); S. Nosé, J. Chem. Phys. **81**, 511 (1984).